2D X-ray spectrometer on WEST: diffracting crystal study and first temperature profiles

Adrien Da Ros, Didier Vezinet, Gilles Colledani, F. Bombarda, V. de Leo

To cite this version:

Adrien Da Ros, Didier Vezinet, Gilles Colledani, F. Bombarda, V. de Leo. 2D X-ray spectrometer on WEST: diffracting crystal study and first temperature profiles. 48TH EPS CONFERENCE ON PLASMA PHYSICS, Jun 2022, ON LINE, France. cea-03736772

HAL Id: cea-03736772
https://cea.hal.science/cea-03736772

Submitted on 22 Jul 2022

HAL is a multi-disciplinary open access archive for the deposit and dissemination of scientific research documents, whether they are published or not. The documents may come from teaching and research institutions in France or abroad, or from public or private research centers.

L'archive ouverte pluridisciplinaire **HAL**, est destinée au dépôt et à la diffusion de documents scientifiques de niveau recherche, publiés ou non, émanant des établissements d'enseignement et de recherche français ou étrangers, des laboratoires publics ou privés.

2D X-ray spectrometer on WEST: diffracting crystal study and first temperature profiles

A. Da Ros[1], D. Vezinet[1], G. Colledani[1], F. Bombarda[2], V. De Leo[2] and the WEST Team[3]

[1] CEA, IRFM, F-13108 Saint Paul-lez-Durance, France

[2] ENEA-FSN, Frascati (Rome), Italy

[3] See (http://west.cea.fr/WESTteam) for the WEST Team (adrien.daros@cea.fr)

Introduction

A 2D X-ray spectrometer with imaging crystals is operated on WEST tokamak. [1]
3 sets of Bragg crystals are mounted on a rotating table [2].

LOS-integrated measurements:
- Te : line intensity ratio
- Ti : Doppler broadening
- Vi : Doppler shift

➢ C3/C4 campaigns data: influence of the half-crystals defects

➢ C5 campaign data: impacts of polluting spectral lines on Te profiles

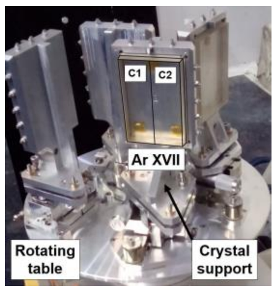

Fig. 1: Rotating table equipped with Ar XVII crystal showed here made in 2 halves

Experimental set-up and Ar XVII spectra

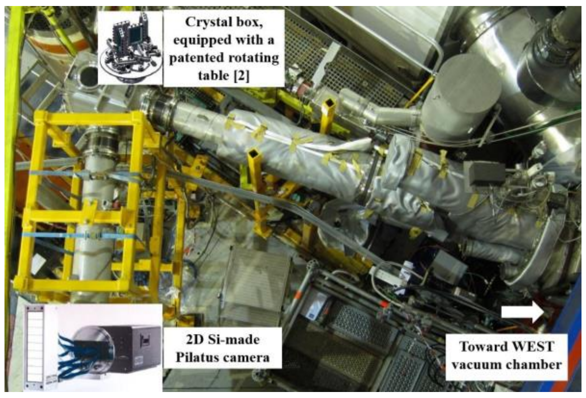

Fig. 2: Top view picture of the XICS spectrometer on WEST

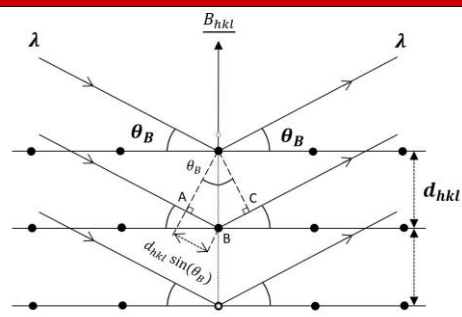

Bragg relation: $n\lambda = 2d_{hkl}.\sin(\theta_B)$

Fig. 3: Sketch of the diffraction process on a Bragg crystal of inter-reticular spacing d_{hkl}

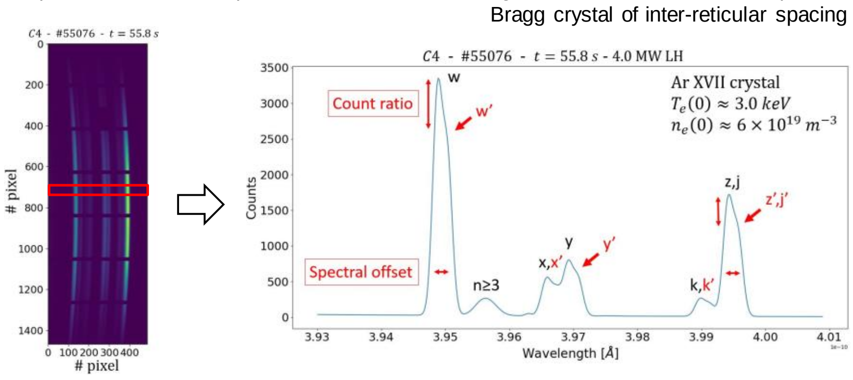

Fig. 4: Example of 2D spectra picture (left column), extracted 1D spectra (right column), showing a line-doubling phenomena (red arrows) doubling all spectral lines recorded, characterized by a **count ratio** and a **spectral offset**

Aim: understand both causes and effects of the spectral offset & the count ratio.

Numerical diffraction profiles

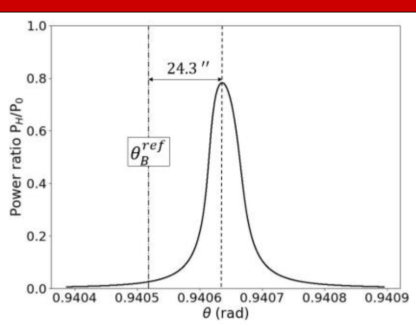

Fig. 5: Computed diffraction pattern for a Quartz Bragg crystal at the resonance line **w** versus diffracting angles θ. [3]

2 issues can affect the diffraction pattern :
- A miscut angle α between optical surface and reticular planes
- Ambiant temperature changes : $d_{hkl}(T) \propto \Delta T$ [4]

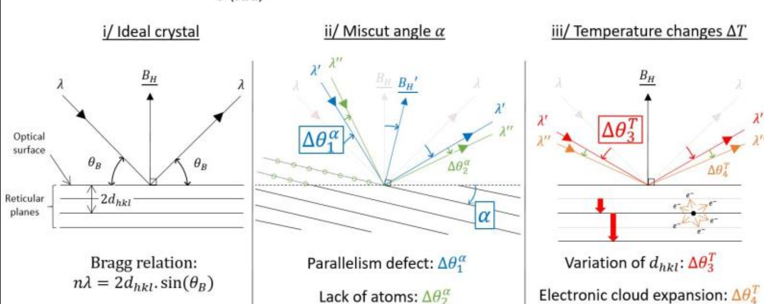

Fig. 6: Induced angular offsets on the direction of diffraction by α and ΔT.

Order of magnitude : $\Delta\theta_1^\alpha \approx \Delta\theta_3^T \gg \Delta\theta_2^\alpha > \Delta\theta_4^T$

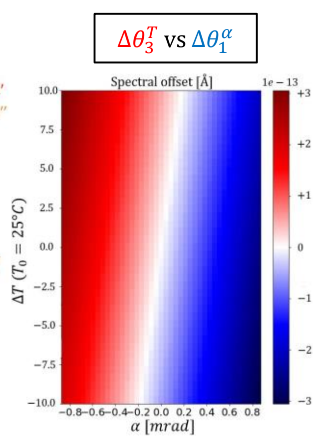

Fig. 7: 2D map of the computed angular offset versus $\Delta\theta_1^\alpha$ and $\Delta\theta_3^T$ variations.

⇒ $\Delta\theta_1^\alpha$ & $\Delta\theta_3^T$ are the main angular offset components.

⇒ Same order of magnitude as fitted with experimental data?

Modelling lines on XICS synthetic diagnostic

Fig. 8: Modelled resonance **w** line positions, diffracted with both Ar XVII half-crystals (*C1* and *C2*), with specified α and ΔT, for the XICS synthetic diagnostic, and comparison with pixel offset recorded from a C4 experimental spectrum.

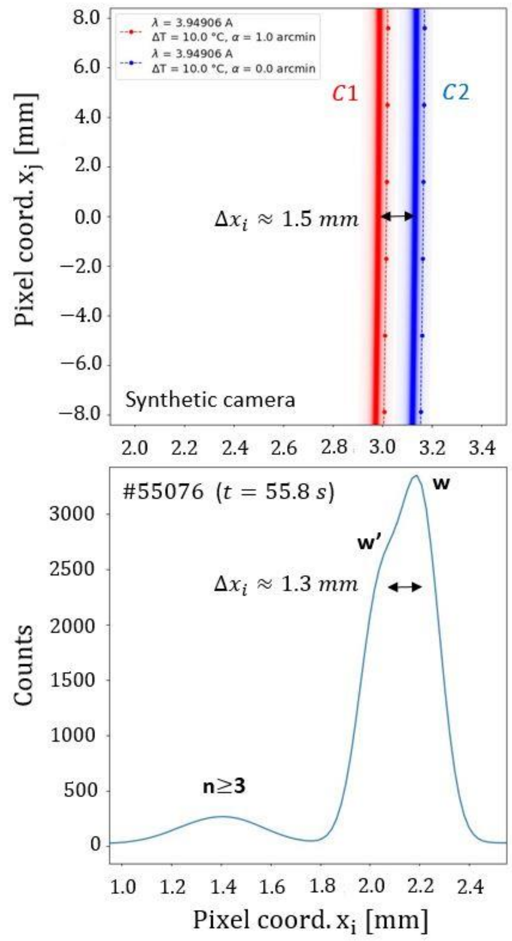

From Fig. 8:

1. Same temperature : $\Delta T = 10°C$
2. Half-crystal 1 : $\alpha = 1.0'$
3. Half-crystal 2 : $\alpha = 0.0'$

➢ $\Delta x_i \approx 1.5 \times 10^{-3}\ m$
$\sim 10^{-3}\ m = \Delta x_i^{w/w'}$
$(\approx \Delta x_{i_{x/y}})$

⟹ Good agreement between :
- i. the modelling of spectral lines under α and ΔT
- ii. the spectral offset fitted from the experimental spectra.

⟹ No apparent link between these sources of error and the count ratio issue.

Electronic temperature profiles

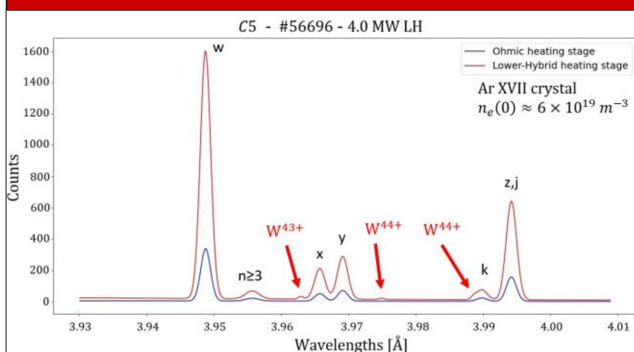

Fig. 9: Spectra from Ar XVII crystal w/o line-doubling

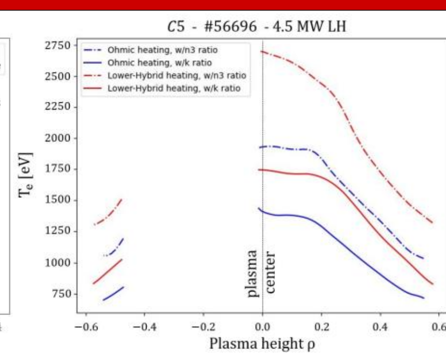

Fig. 10: Te LOS-profiles, for Ohmic and Lower Hybrid heating stages, from the resonance line **w** to the dielectronic satellite **k** line ratio and to **n ≥ 3** satellites line ratio

- 2 consecutive plasma heating stages: $P_{Ohm}(0.5\ MW) < P_{LH}(4.5\ MW)$

➢ At low power, temperature plateaus reached at the plasma center

➢ At high power, $T_{e,w/k}\ (0 < \rho < 0.2) = 1.8\ keV$ ⇒ saturated
$T_{e,w/n3}\ (\rho = 0) = 2.7\ keV$ ⇒ no issue noticed

⟹ Disagreement between **w/k** and **w/n3** line ratios due to polluting W lines [5], next to the Ar Li-like satellite line **k**.

Conclusion

- Line-doubling phenomena due to different structural properties of half-crystals; Computation of the diffracting pattern of a Bragg crystal, depending on:
  - ➢ The parallelism defect between the optical surface and reticular planes;
  - ➢ The ambient temperature to which the crystal is subject.

⇒ Better understanding of the spectral offset ⇒ improve synthetic diagnostic

- With or w/o this issue, presence of some polluting W lines (on Ar XVII spectra) affecting the measured intensity of the **k** lines ⇒ errors on Te profiles

In the next months:
- Identify the causes of the count ratio comparing all plasma campaigns data;
- Identify accurately the polluting spectral lines, especially the W lines in Ar spectra.

References

[1] D. Vezinet et al, ECPD conference; Lisboa, 2019, poster P3.6
[2] G. Colledani, patent number 1653710 from the 27th April 2016
[3] R. Bartiromo, F. Bombarda et al., Nucl. Instrum. Methods Phys. Res. A 221, 453 (1984)
[4] L. Delgado-Aparicio et al., Plasma Phys. Control. Fusion 55, 125011 (2013)
[5] J. E. Rice et al., J. Phys. B: At. Mol. Opt. Phys., 54 095701 (2021)